

Microstructure Evolution of a High Zinc Containing Al-Zn-Mg-Cu Alloy during Homogenization

Wen Kai¹, Xiong Baiqing¹, Zhang Yongan¹, Wang Guojun², Li Xiwu¹, Li Zhihui¹,
Huang Shuhui¹, Liu Hongwei¹

¹State Key Laboratory of Non-ferrous Metals and Processes, General Research Institute for Non-ferrous Metals, Beijing 100088, China;

²Northeast Light Alloy Co. Ltd, Harbin 150060, China

Abstract: The microstructural evolution of a high Zn-containing Al-Zn-Mg-Cu alloy during homogenization was investigated by optical microscopy, differential scanning calorimetry, scanning electron microscope and X-ray diffraction. A homogenization kinetic equation derived from a diffusion kinetic model was established to confirm the optimum homogenization parameter. Results indicate that severe segregation exists in the as-cast alloy. The non-equilibrium eutectics consist of $\alpha(\text{Al})$, $\text{Mg}(\text{Zn}, \text{Cu}, \text{Al})_2$, $\text{S}(\text{Al}_2\text{CuMg})$, $\theta(\text{Al}_2\text{Cu})$ and Fe-enriched phases. In the present work, no transformation from $\text{Mg}(\text{Zn}, \text{Cu}, \text{Al})_2$ to $\text{S}(\text{Al}_2\text{CuMg})$ phases occurs during homogenization and $\text{Mg}(\text{Zn}, \text{Cu}, \text{Al})_2$ phases directly dissolve into the matrix. $\theta(\text{Al}_2\text{Cu})$ phases dissolve into the matrix while Fe-enriched phases still exist after homogenization. In addition, the contents of Zn and Mg elements in Fe-enriched phases are reduced or even disappear by prolonging the holding time of homogenization. The proper homogenization parameter is 440 °C/12 h + 468 °C/24 h, which is in consistent with the results of homogenization kinetic analysis.

Key words: Al-Zn-Mg-Cu alloy; microstructure; homogenization; phase transformation

Al-Zn-Mg-Cu alloys have been extensively used in aerospace structures, automobile manufacturing and advanced weapon systems due to their high strength and improved resistance to fracture^[1]. Usually, Al-Zn-Mg-Cu alloys with higher Zn amount have better mechanical properties^[2]. However, more micro-segregation and coarse intermetallic particles are formed during solidification, which deteriorate fracture and fatigue performances^[3-5]. It is well known that micro-segregation can be eliminated and soluble intermetallic particles can dissolve into the matrix during homogenization^[6-9]. Hence, homogenization treatment is an important procedure to obtain a good service performance.

The contents of alloying elements in Al-Zn-Mg-Cu alloys are high and phases in as-cast microstructure are abundant and complicated, including $\text{Mg}(\text{Zn}, \text{Cu}, \text{Al})_2$, $\eta(\text{MgZn}_2)$, $\text{S}(\text{Al}_2\text{CuMg})$, $\theta(\text{Al}_2\text{Cu})$ and Fe-rich phases^[3,10-12]. Moreover,

$\text{S}(\text{Al}_2\text{CuMg})$ phase can be obtained by the transformation of $\text{Mg}(\text{Zn}, \text{Cu}, \text{Al})_2$ phase during homogenization. Deng et al^[7] found that $\text{Mg}(\text{Zn}, \text{Cu}, \text{Al})_2$ phase transformed into $\text{S}(\text{Al}_2\text{CuMg})$ phase during homogenization in Al-5.87Zn-2.07Mg-2.28Cu alloy. A similar conclusion was obtained by Li^[13], Fan^[3] and Lv^[14]. However, the study of Xiao^[15] showed that no transformation was observed after 470 °C/24 h homogenization in Al-8.1Zn-2.05Mg-2.3Cu alloy. Liu^[2] and Li^[16] got the same result as Xiao^[15]. Recently, Liu^[2] asserted that the transformation from $\text{Mg}(\text{Zn}, \text{Cu}, \text{Al})_2$ to $\text{S}(\text{Al}_2\text{CuMg})$ phase was very hard when Zn content was higher than 8 wt%. Literatures indicated that phase dissolution and transformation can be affected by alloying elements ratio and heat treatment processing^[2].

In the present paper, phase transformation during homogenization was studied and a diffusion kinetic model was employed to verify the preferential homogenization

Received date: April 25, 2016

Foundation item: National Key Basic Research Development Program of China (2012CB619504); National Natural Science Foundation of China (51274046)

Corresponding author: Xiong Baiqing, Ph. D., Professor, State Key Laboratory of Non-ferrous Metals and Processes, General Research Institute for Nonferrous Metals, Beijing 100088, P. R. China, Tel: 0086-10-62055404, E-mail: xiongbq@grinm.com

Copyright © 2017, Northwest Institute for Nonferrous Metal Research. Published by Elsevier BV. All rights reserved.

parameter. The influence of Zn content on $S(\text{Al}_2\text{CuMg})$ phase formation was explored theoretically. In addition, diffusion activation energy and frequency factor of Zn element were employed to analyze the effect of Zn content on diffusion coefficient during homogenization.

1 Experiment

The chemical composition of the billet with a diameter of 220 mm used in the present study was: Al-9.79Zn-2.17Mg-1.94Cu-0.10Zr-0.056Fe-0.028Si (wt%). Specimens for microstructural analysis were extracted from near the mid-radius of the billet. Homogenization treatments were conducted in air using a resistance heated box furnace with forced air convection. Two-stage homogenization was employed. The first stage was 440 °C/12 h and the second stage chose 460, 465, 468 and 470 °C with a series of soaking time. Microstructures were observed using an optical microscope (OM) for the as-cast and as-homogenized conditions. The composition of large intermetallic particles was obtained by energy dispersive X-ray spectroscopy (EDS) attached to a JEOL JSM 7001F scanning electron microscope (SEM). The microstructural characterization of the as-cast specimens was carried out by X-ray diffraction (XRD), Rigaku D/Max 2500 diffractometer, and 0.5 deg step. The melting temperature associated with the constituent particles in the as-cast specimen was measured by differential scanning calorimetry (DSC) conducted on NETZSCH STA 409C/CD instrument with a heating rate of 10 K/min ranging from room temperature to 550 °C.

2 Results and Discussion

2.1 Microstructure and DSC analysis of as-cast Al-Zn-Mg-Cu alloy

Non-equilibrium eutectics and intermetallics mainly precipitated on the grain boundaries and interdendritic spaces during the final stage of solidification. Composition segregation of dendritic structure came into being micro-battery, downgrading electrochemical corrosion resistance^[17]. The microstructure of the as-cast alloy is given in Fig.1. The coarse black phases form a sort of netty structure (Fig.1a) and lamellar structure is observed (Fig.1b).

XRD pattern of as-cast Al-Zn-Mg-Cu alloy is shown in Fig.2. The main phases in as-cast Al-Zn-Mg-Cu alloy are $\alpha(\text{Al})$ and the phases with the crystal structure of MgZn_2 ^[2]. Typical phases of as-cast Al-Zn-Mg-Cu alloy are shown in Fig.3. EDS results (Table 1) reveal that white phases (A and D points in Fig.3) may be $\text{Mg}(\text{Zn}, \text{Cu}, \text{Al})_2$ phases. Fe element is detected by EDS (B point in Fig.3a), indicating that it is Fe-enriched phase. The light grey phase (C point in Fig.3a) contains a little Zn and Mg elements, and the composition is close to stoichiometric Al_2Cu . Similarly, the dark gray phases (E and F points in Fig.3b) are considered

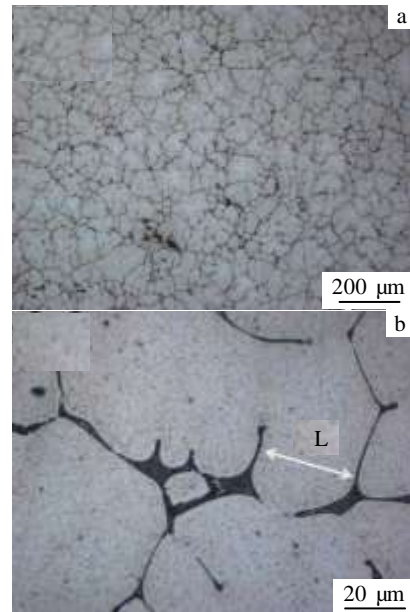


Fig.1 OM micrographs of the as-cast alloy

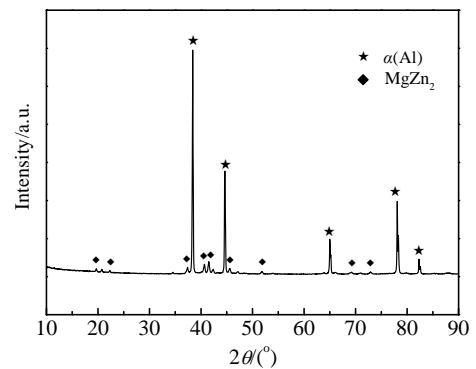


Fig.2 XRD pattern of the as-cast alloy

as $S(\text{Al}_2\text{CuMg})$ phase. So the second phases consist of $\text{Mg}(\text{Zn}, \text{Cu}, \text{Al})_2$, $S(\text{Al}_2\text{CuMg})$, $\theta(\text{Al}_2\text{Cu})$ and Fe-enriched phases.

DSC curve of as-cast Al-Zn-Mg-Cu alloy is shown in Fig. 4. It could be clearly seen from the figure that inflection point is 472.0 °C. The study of Xu^[18] declared that this temperature could be considered as the melting temperature of $\text{Mg}(\text{Zn}, \text{Cu}, \text{Al})_2$ phase. In practice, this method is not sufficiently accurate. If the melting temperature was underestimated, lower homogenization temperature would be inefficient for dissolving soluble constituents. If it was overestimated, overheating might occur, resulting in the formation of detrimental overheated holes. Thus, considering the first step homogenization was for obtaining Al_3Zr dispersoid particles, a series of experiments with

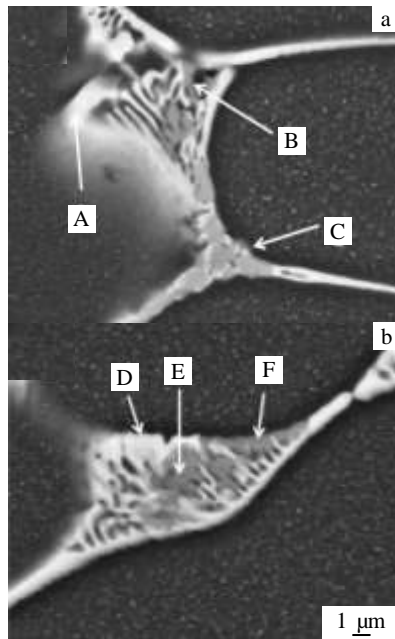


Fig.3 SEM backscattered electron images of the as-cast alloy

Table 1 EDS analysis results of arrow positions in Fig.3 (at%)

Position	Al	Zn	Mg	Cu	Fe
A	48.75	19.92	24.21	17.11	-
B	55.96	4.04	21.26	15.80	2.94
C	73.00	2.31	2.42	22.27	-
D	41.26	25.29	25.42	18.03	-
E	58.49	6.49	21.14	13.88	-
F	68.41	3.80	16.59	11.00	-

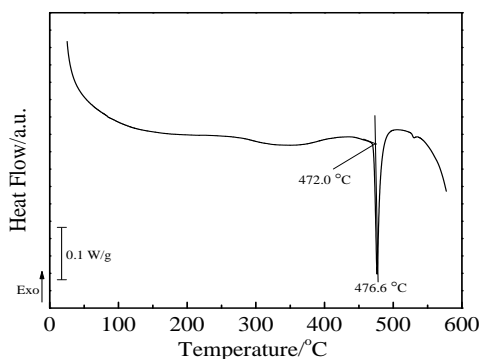


Fig.4 DSC curve of the as-cast alloy

different second step homogenization temperature around 472.0 °C were carried out to acquire proper homogenization parameter.

2.2 Homogenization of the Al-Zn-Mg-Cu alloy

The first stage of homogenization treatment aims to

acquire fine Al_3Zr dispersoid particles, which significantly pin grain boundary so as to inhibit recrystallization of subsequent processes. Robson^[19] proposed that the maximum nucleation rate was obtained between 420 and 450 °C. Considering the first stage homogenization regime employed in literatures and industrial production situation, the alloy was homogenized at 440 °C for 12 h.

Different temperatures (460, 465, 468 and 470 °C) with various soaking time are chose as second stage homogenization parameters with a heating up interval of 2 h since 440 °C. The Fe-enriched phases are not eliminated by homogenization treatment. No $\theta(\text{Al}_2\text{Cu})$ and $\text{S}(\text{Al}_2\text{CuMg})$ phases are observed after homogenization. According to SEM and EDS observation, various parameters of second stage homogenization treatment are labelled as “Y” for the solely existence of Fe-enriched phases and “N” for the persistence of $\text{Mg}(\text{Zn,Cu,Al})_2$ phase. The details are displayed in Table 2.

The results show that $\text{Mg}(\text{Zn, Cu, Al})_2$ phase still exists till 48 h of the second stage homogenization processed at 460 °C. And slightly overburning structure is observed in the specimen processed at 470 °C. The microstructure evolution with a second stage homogenization temperature of 468 °C is shown in Fig.5. A mass of $\text{Mg}(\text{Zn, Cu, Al})_2$ phase exists along the boundary after processed at 440 °C for 12 h (Fig.5a), which is still observed after 6 h of the second stage homogenization (Fig.5b) and then diminishes after 12 h (Fig.5c). The residual black phase on the boundary after 18 h (Fig.5d) is verified as Fe-enriched phases and no $\text{Mg}(\text{Zn, Cu, Al})_2$ phase is observed. The grain size after 24 h (Fig.5e) grows slightly compared with that after 18 h. Besides, no $\text{S}(\text{Al}_2\text{CuMg})$ phase is observed after all homogenization parameters. Based on literature, the processing temperatures employed in the present work are not enough for $\text{S}(\text{Al}_2\text{CuMg})$ phase dissolution, so $\text{Mg}(\text{Zn, Cu, Al})_2$ phase directly dissolves into the matrix without transforming to $\text{S}(\text{Al}_2\text{CuMg})$ phase.

The phase evolution in homogenized alloy is presented in Fig.6. EDS analysis (Table 3) reveals that Zn and Mg elements exist in Fe-enriched phases of the specimen homogenized at 468 °C for 12 and 24 h, but diminish for 36 and 48 h. This indicates that Fe-enriched phases could not dissolve into the matrix with a second stage homogenization

Table 2 Phase dissolution of the alloy with various second stage homogenization temperatures

Temperature/ °C	Soaking time/h			
	≥12	≥18	≥24	≥48
460	N	N	N	N
465	N	N	Y	-
468	N	Y	-	-
470	Y	-	-	-

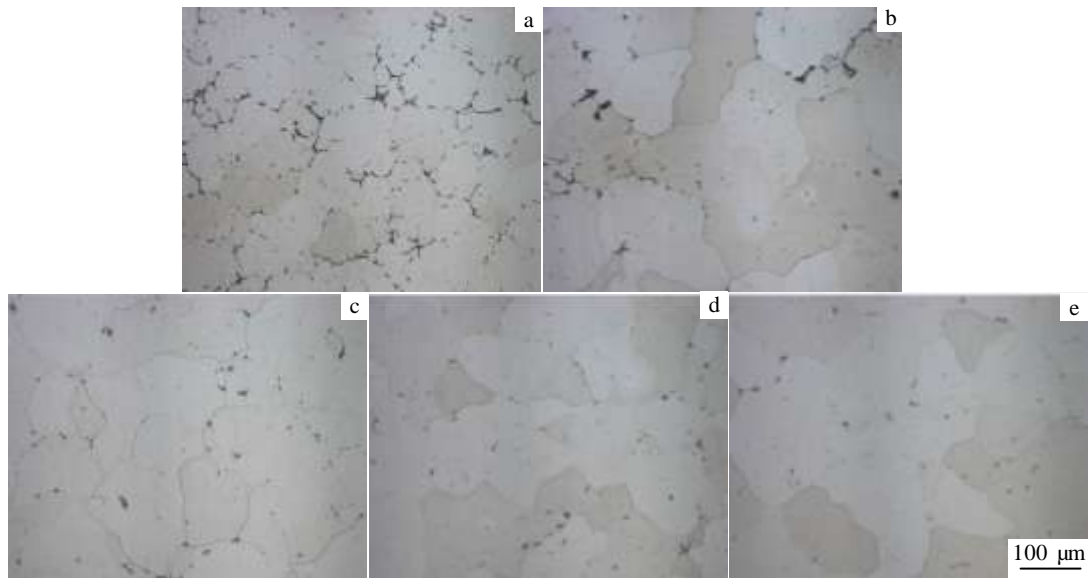


Fig.5 Microstructure evolution process of the as-homogenized alloy: (a) 440 °C/12 h, (b) 440 °C/12 h + 468 °C/6 h, (c) 440 °C/12 h + 468 °C/12 h, (d) 440 °C/12 h + 468 °C/18 h, and (e) 440 °C/12 h + 468 °C/24 h

temperature of 468 °C, but Zn and Mg elements in Fe-enriched phases could diffuse into the matrix over homogenization time.

A proper heat treatment regime may meet non-overburning, treatment temperature as high as possible and maximum soluble components dissolving into the matrix. The billet under industrial processing has asynchronous heating from edge to center. In the present work, the preferential homogenization process is 440 °C/12 h + 468 °C/24 h for the alloy.

2.3 Parameter verification by a diffusion kinetic model

The main phase that dissolved into the matrix during homogenization is $Mg(Zn, Cu, Al)_2$ phase^[16,20]. The line scanning analysis of eutectic structure (Fig.7) indicates that segregation of Zn, Mg and Cu elements exists along eutectic structure on grain boundaries. Because the diffusion coefficient of Cu element is much lower than that of Mg and Zn during homogenization. Therefore, the homogenization process is considered to be effectively controlled by the diffusion of Cu element. According to Liu^[2] and Deng^[7], the homogenization kinetic equation was given as:

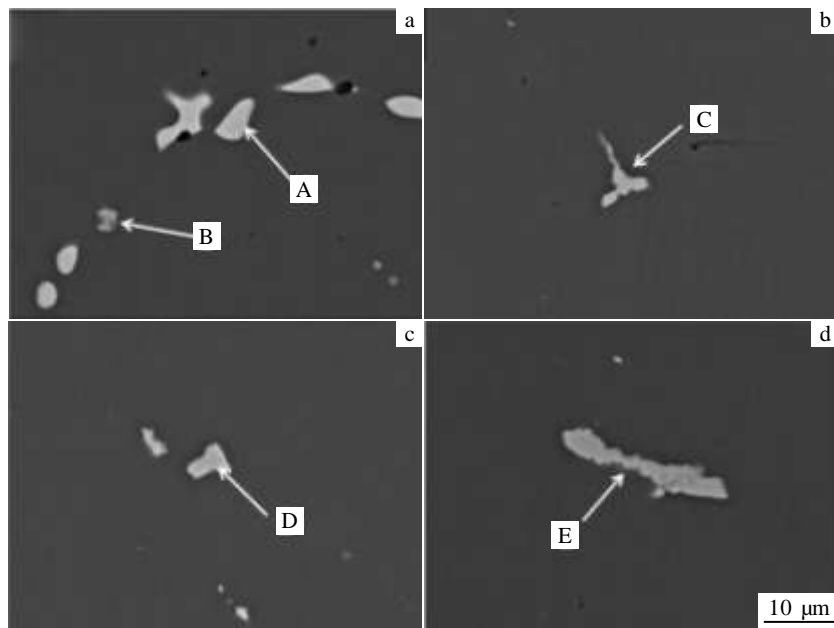


Fig.6 SEM backscattered electron images of the as-homogenized alloy: (a) 440 °C/12 h + 468 °C/12 h, (b) 440 °C/12 h + 468 °C/24 h, (c) 440 °C/12 h + 468 °C/36 h, and (d) 440 °C/12 h + 468 °C/48 h

Table 3 EDS analysis results of arrow positions in Fig.6 (at%)

Position	Al	Zn	Mg	Cu	Fe
A	28.24	23.48	31.11	17.16	-
B	76.19	1.54	1.45	14.27	6.55
C	72.23	1.59	0.78	17.51	7.88
D	75.43	-	-	16.70	7.88
E	81.11	-	-	13.30	5.59

$$\exp\left(-\frac{4\pi^2 Dt}{L^2}\right) = \frac{1}{100} \quad (1)$$

According to Arrhenius equation

$$D = D_0 \exp\left(-\frac{Q}{RT}\right) \quad (2)$$

where T , t and L are homogenization temperature, soaking time and interdendritic spacing, respectively; R , Q and D_0 are the gas constant ($8.314 \text{ J}\cdot\text{mol}^{-1}\cdot\text{K}^{-1}$), diffusion activation energy and frequency factor, respectively.

A hypothesis was introduced in which the diffusion coefficient was an exponential function that depended on temperature. According to the study of Xie^[21], the diffusion coefficient of Cu element was

$$D(\text{Cu}) = 4.8 \times 10^{-5} \exp(-16069/T) \quad (3)$$

so Eq.(1) can be written as

$$4.11 \times 10^{-4} t \exp(-16069/T) = L^2 \quad (4)$$

In the present work, as marked in Fig.5a, the interdendritic spacing (L) of as-cast Al-Zn-Mg-Cu alloy was measured by optical microscope. Hundreds of data were collected to get a statistical distribution of interdendritic spacing. The results are presented in Fig.8. Apparently, most spacing (L) concentrates upon the interval of 30~100 μm . Hence, the results were employed as the spacing distribution of the specimen processed after 440 $^{\circ}\text{C}/12 \text{ h}$ homogenization. Substituting hour (h) and Celsius ($^{\circ}\text{C}$), Eq.(4) could be written as

$$T = 16069 / \ln\left(\frac{1.4796}{L^2} t\right) - 273.15 \quad (5)$$

Then the homogenization kinetic curves for different interdendritic spacing were obtained, as shown in Fig.9.

It is concluded from Fig.8 that larger $\text{Mg}(\text{Zn}, \text{Cu}, \text{Al})_2$ phase spacing (L) corresponds to longer soaking time under uniform processing temperature. For $T = 468 \text{ }^{\circ}\text{C}$ and $L=100 \mu\text{m}$, t is 17.6 h. So the element distribution is homogeneous after processing for 18 h. The experimental results (Table 2) show that no $\text{Mg}(\text{Zn}, \text{Cu}, \text{Al})_2$ phase is detected after this process. Considering thermal-uniformity of the billet, the model has verified the adequacy of homogenization parameter of 440 $^{\circ}\text{C}/12 \text{ h} + 468 \text{ }^{\circ}\text{C}/24 \text{ h}$.

2.4 Theoretical analysis on no $\text{S}(\text{Al}_2\text{CuMg})$ phase transformation

As observed in traditional Al-Zn-Mg-Cu alloys with low

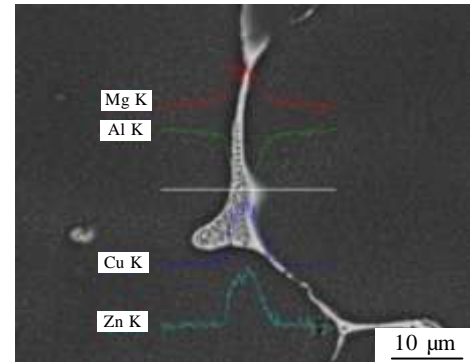


Fig.7 Eutectic structure and element Mg, Al, Cu and Zn line scanning of the as-cast alloy

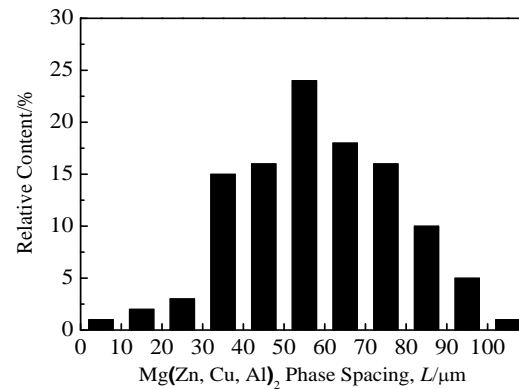


Fig.8 $\text{Mg}(\text{Zn}, \text{Cu}, \text{Al})_2$ phase spacing of the as-cast alloy

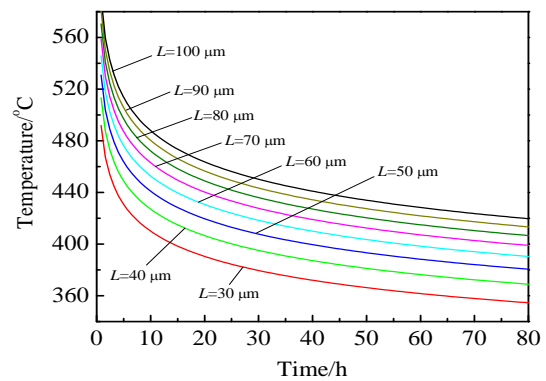


Fig.9 Homogenization kinetic curves of the alloy with different $\text{Mg}(\text{Zn}, \text{Cu}, \text{Al})_2$ phase spacings

Zn content, such as alloys studied by Fan^[3], Deng^[7] and Li^[13] with Zn content (wt%) of 6.31, 5.87 and 6.3, respectively, $\text{S}(\text{Al}_2\text{CuMg})$ phase was observed to be transformed from $\text{Mg}(\text{Zn}, \text{Cu}, \text{Al})_2$ phase during homogenization. According to the work of Xie^[21], calculation equations of solid diffusion coefficient of Zn, Mg and Cu elements were deduced and are shown in Table 4. The diffusion rate of Zn element is much higher than that of Mg and Cu elements at the same

temperature. As homogenization continues, the reduction of Zn content and the accumulation of Cu content make the constituent of this area in accordance with S(Al₂CuMg) phase. Finally, S(Al₂CuMg) phase appears.

Because temperature variation significantly affects diffusion coefficient, previous work used the temperature-dependent hypothesis. Actually, diffusion coefficient is also influenced by component variation. The intrinsic driving force of diffusion is the concentration gradient to alloys. The component difference between Mg(Zn, Cu, Al)₂ phase and the matrix is reduced over homogenization, leading to shrinking concentration gradient accounting for degraded diffusion coefficient. So the diffusion coefficient could be written as^[22]:

$$D = gfv a^2 \exp\left(\frac{\Delta S}{k}\right) \exp\left(-\frac{\Delta H}{kT}\right) \quad (6)$$

where ΔS and ΔH are vacancy diffusion activation entropy and enthalpy for interstitial diffusion, respectively; g , a , v , f and k are geometrical factor, lattice parameter, attempt frequency, correlation factor and Boltzmann constant, respectively.

According to the pioneering work of Robson and Prangnell^[19]

$$\Delta S = \lambda \theta \frac{\Delta H}{T_m} \quad (7)$$

here λ is a constant that depends on the structure and on the diffusion mechanism, θ is a constant whose values lies between -0.25 to -0.45 for most metals, and T_m is the melting temperature, in the present work, referred to Mg(Zn, Cu, Al)₂ phase.

Table 4 Solid diffusion coefficient of Cu, Mg and Zn atom during homogenization (m²/s)

Element	Calculation equation ^[22]	Temperature ($T-273.15$)/ °C				
		440	460	465	468	470
Cu	$D=4.8 \times 10^{-5} \exp(-16069/T)$	7.862×10^{-15}	1.454×10^{-14}	1.686×10^{-14}	1.842×10^{-14}	1.952×10^{-14}
Mg	$D=6.23 \times 10^{-6} \exp(-13831/T)$	2.353×10^{-14}	3.994×10^{-14}	4.539×10^{-14}	4.896×10^{-14}	5.149×10^{-14}
Zn	$D=2.45 \times 10^{-5} \exp(-14385/T)$	4.256×10^{-14}	7.378×10^{-14}	8.427×10^{-14}	9.119×10^{-14}	9.608×10^{-14}
$D_{Cu}:D_{Mg}:D_{Zn}$		1:3.0:5.4	1:2.7:5.1	1:2.7:5.0	1:2.7:5.0	1:2.6:4.9

to S(Al₂CuMg) phase was very difficult when Zn content was higher than 8 wt%. It may be inferred that the diffusion coefficient of Zn element suffers a slowdown with the increment of Zn content. As a result, no S(Al₂CuMg) phase transformation occurs during homogenization in the alloy. In the present work, no θ (Al₂Cu) phase is observed after homogenization. Literature showed that the melting point of θ (Al₂Cu) phase was not less than 500 °C. Similar results were reported by the study of Mondal^[23] on 7055 aluminum alloy. In the present work, the θ (Al₂Cu) phase contains Zn and Mg elements, which is not strictly stoichiometric Al₂Cu and the melting temperature is degraded. In addition, Cu content in the matrix is really low, and the concentration gradient between Cu-enriched phases and the matrix is fairly big, leading to a high diffusion driving force. The schematic of diffusion coefficient of zinc versus zinc content is shown in Fig.10 which could vividly describe the mechanism.

Then the frequency factor could be written as:

$$D_0 = gfv a^2 \exp\left(\frac{\lambda \theta \Delta H}{kT_m}\right) \quad (8)$$

Hence, the frequency factor is positively correlated with activation enthalpy while the exponential term of Eq.(8) is negatively correlated. Activation enthalpy is affected by interatomic bonding force, which means that the tighter interatomic bonding force leads to higher activation enthalpy.

For Al-Zn-Mg-Cu alloys with low Zn content, the increasing concentration of Zn leads to a higher percentage of Al-Zn bonds. The binding energy of Al-Zn bond is weaker than that of Al-Al, Al-Mg and Al-Cu bonds, so the increment of Al-Zn bond degrades the energy barrier of interchange between Zn atoms and vacancies. Thereupon the activation enthalpy is reduced which results in a decrement of frequency factor and an increment of the exponential term. The comprehensive consequence is an enhancement of diffusion coefficient. Therefore, the diffusion of Zn atom meets the formation condition of S(Al₂CuMg) phase.

The calculated results in Table 4 show that the diffusion coefficient of Zn element is almost five times bigger than that of Cu element. In fact, the diffusion coefficient of Zn element in high Zn containing Al-Zn-Mg-Cu alloys is greatly decreased to the extent that it has no significant advantage to Cu element. So it is rather difficult to match the element proportion to form S(Al₂CuMg) phase. As mentioned above, Liu^[2] asserted that the phase transition from Mg(Zn, Cu, Al)₂

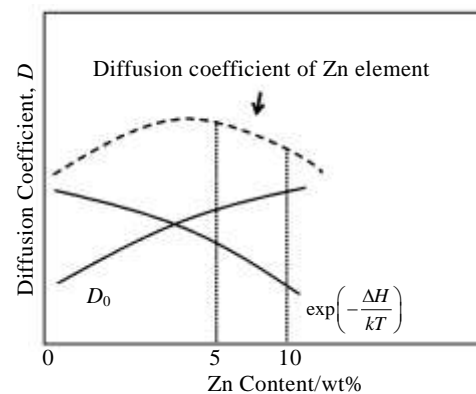


Fig.10 Schematic of diffusion coefficient of Zn element versus Zn content of Al-Zn-Mg-Cu alloys

3 Conclusions

1) Severe dendritic segregation exists in as-cast microstructure of the high Zn-containing Al-Zn-Mg-Cu alloy. The second phases in the Al-Zn-Mg-Cu alloy consist of Mg(Zn, Cu, Al)₂, S(Al₂CuMg), θ (Al₂Cu) and Fe-enriched phases.

2) The Mg(Zn, Cu, Al)₂ phase directly dissolves into the matrix without transforming to S(Al₂CuMg) phase during homogenization. The diffusion rate of Zn element in Mg(Zn, Cu, Al)₂ phase has no significant advantage to that of Mg and Cu elements during homogenization, which could not match the element proportion to form S(Al₂CuMg) phase.

3) θ (Al₂Cu) phase dissolves into the matrix due to the degraded melting temperature resulting from containment of Zn and Mg elements. Zn and Mg elements in Fe-enriched phases dissolve into the matrix over homogenization time.

4) The optimized homogenization parameter is 440 °C/12 h + 468 °C/24 h, which is consistent with the results of homogenization kinetic curves.

References

- Wang Haijun, Xu Ju, Kang Yonglin et al. *Journal of Alloys and Compounds*[J], 2014, 585: 19
- Liu Yan, Jiang Daming, Xie Wenlong et al. *Materials Characterization*[J], 2014, 93(7): 173
- Fan Xigang, Jiang Daming, Meng Qingchang et al. *Materials Letters*[J], 2006, 60(12): 1475
- Li Wenbin, Pan Qinglin, Xiao Yanping et al. *Transactions of Nonferrous Metals Society of China*[J], 2011, 21(10): 2127
- Wu Lingmei, Wang Wenhsung, Hsu Yungfu et al. *Journal of Alloys and Compounds*[J], 2008, 456(1): 163
- Han N M, Zhang X M, Liu S D et al. *Journal of Alloys and Compounds*[J], 2011, 509(10): 4138
- Deng Ying, Yin Zhimin, Cong Fuguan. *Intermetallics*[J], 2012, 26: 114
- Senkov O N, Shagiev M R, Senkova S V et al. *Acta Materialia*[J], 2008, 56(15): 3723
- Liu S D, You J H, Zhang X M et al. *Materials Science and Engineering A*[J], 2010, 527(4-5): 1200
- Liu Juntao, Zhang Yongan, Li Xiwu et al. *Rare Metals*[J], 2016, 35(5): 380
- Liu S D, Yuan Y B, Li C B et al. *Metals and Materials International*[J], 2012, 18(4): 679
- Zheng Yunlin, Li Chengbo, Liu Shengdan et al. *Transactions of Nonferrous Metals Society of China*[J], 2014, 24(7): 2275
- Li Niankui, Cui Jianzhong. *Transactions of Nonferrous Metals Society of China*[J], 2008, 18(4): 769
- Lv Xinyu, Guo Erjun, Li Zhihui et al. *Rare Metals*[J], 2011, 30(6): 664
- Xiao Yanping, Pan Qinglin, Li Wenbin et al. *Journal of Materials Science and Engineering*[J], 2010, 28(6): 920 (in Chinese)
- Li Hai, Cao Dahu, Wang Zhixiu et al. *Journal of Materials Science*[J], 2008, 43(5): 1583
- Xu D K, Birbilis N, Rometsch P A. *Corrosion: the Journal of Science and Engineering*[J], 2012, 68(3): 0 350 011
- Xu D K, Rometsch P A, Birbilis N. *Materials Science and Engineering A*[J], 2012, 534: 234
- Robson J D, Prangnell P B. *Acta Materialia*[J], 2001, 49(4): 599
- Zuo Yuting, Wang Feng, Xiong Baiqing et al. *The Chinese Journal of Nonferrous Metals*[J], 2010, 20(5): 820 (in Chinese)
- Xie Fanyou, Yan Xinyan, Ding Ling et al. *Materials Science and Engineering A*[J], 2003, 355(1-2): 144
- Mehrer H. *Diffusion in Solids: Fundamentals, Methods, Materials, Diffusion-Controlled Processes*[M]. Heidelberg: Springer-Verlag, 2007: 32
- Chandan Mondal, Mukhopadhyay A K. *Materials Science and Engineering A*[J], 2005, 391(1-2): 367

高 Zn 含量 Al-Zn-Mg-Cu 合金均匀化过程中显微结构演变研究

温 凯¹, 熊柏青¹, 张永安¹, 王国军², 李锡武¹, 李志辉¹, 黄树晖¹, 刘红伟¹

(1. 北京有色金属研究总院 有色金属材料制备加工国家重点实验室, 北京 100088)

(2. 东北轻合金有限责任公司, 黑龙江 哈尔滨 150060)

摘要: 对一种高Zn含量Al-Zn-Mg-Cu合金进行均匀化处理, 通过光学显微镜(OM)、差热分析(DSC)、扫描电镜(SEM)和X射线衍射(XRD)研究合金的显微结构演变。使用扩散动力学模型推导均匀化动力学方程, 用于确认最佳均匀化参数。结果表明: 合金的铸态组织中存在严重偏析, 非平衡共晶结构包含 α (Al)、Mg(Zn, Cu, Al)₂、S(Al₂CuMg)、 θ (Al₂Cu)和富Fe相。当前研究表明均匀化过程中没有发生Mg(Zn, Cu, Al)₂相向S(Al₂CuMg)相的转变, Mg(Zn, Cu, Al)₂相直接回溶。随着均匀化的进行, θ (Al₂Cu)相溶入基体。均匀化后富Fe相仍残留, 但随着保温时间的延长, 富Fe相中的Zn、Mg元素逐渐减少或消失。最佳均匀化参数为440 °C/12 h + 468 °C/24 h, 这与均匀化动力学的分析相一致。

关键词: Al-Zn-Mg-Cu 合金; 显微结构; 均匀化; 相变

作者简介: 温 凯, 男, 1990 年生, 博士生, 北京有色金属研究总院有色金属材料制备加工国家重点实验室, 北京 100088, 电话: 010-82241172, E-mail: wenkai900416@163.com